

1 *Article*

2 **The change in biotic and abiotic soil components influenced**
3 **by paddy soil microbial fuel cells loaded with various**
4 **resistances**

5
6 Williamson Gustave ^{ab}, Zhao-Feng Yuan ^{ab}, Raju Sekar ^c, Yu-Xiang Ren ^a, Hu-Cheng Chang^a
7 and Zheng Chen ^{a*}

8
9
10 ^a Department of Environmental Science, Xi'an Jiaotong-Liverpool University, Suzhou, Jiangsu
11 215123, China

12 ^b Department of Environmental Science, University of Liverpool, Brownlow Hill, Liverpool L69
13 7ZX, United Kingdom

14 ^c Department of Biological Sciences, Xi'an Jiaotong-Liverpool University, Suzhou 215123,
15 China

16 * Corresponding author. Department of Environmental Science, Xi'an Jiaotong-Liverpool
17 University, Suzhou, Jiangsu 215123, China.

18 E-mail address: ebiogeochem@outlook.com or Zheng.Chen@xjtlu.edu.cn (Z. Chen)

19

20 **Abstract:** Soil microbial fuel cells (sMFC) are a novel technique that use organic matters in soils
21 as an alternative energy source. External resistance (ER) is a key factor influencing sMFC
22 performance and, furthermore, alters the soil's biological and chemical reactions. However, little
23 information is available on how the microbial community and soil component changes in sMFC
24 with different ER. Therefore, the effects of anodes of sMFC at different ER (2000 Ω , 1000 Ω , 200
25 Ω , 80 Ω and 50 Ω) were examined by measuring organic matter (OM) removal efficiency, trace
26 elements in porewater and bacterial community structure in contaminated paddy soil. The results
27 indicated that ER has significant effects on sMFC power production, OM removal efficiency and
28 bacterial beta diversity. Moreover ER influences iron, arsenic and nickel concentration as well in
29 soil porewater. In particular, greater current densities were observed at lower ER (2.4mA, 50 Ω)
30 compared to a higher ER (0.3mA, 2000 Ω). The removal efficiency of OM increased with
31 decreasing ER whereas it decreased with soil distance away from the anode. Furthermore, principal
32 coordinate analysis (PCoA) revealed that ER may shape the bacterial communities that develop in
33 the anode vicinity but have minimal effect on that of the bulk soil. The current study illustrates
34 that lower ER can be used to selectively enhance the relative abundance of electrogenic bacteria
35 and lead to high OM removal.

36 **Keywords:** External resistances; Soil microbial fuel cells; Paddy soil; Geobacter; Arsenic; Iron;
37 Organic matter

38

39 1. Introduction

40 Organic carbon in sediments or soils can be used as a new source of energy when employed
41 in microbial fuel cells (MFC). Soil microbial fuel cells (sMFC) are a special type of MFC that
42 produce electricity by using organic chemicals present in soils as energy source [1-4]. In sMFC
43 organic matter (OM) is oxidized at the anode by the soil microorganism, resulting in the production
44 of electrons. The electrons produced during OM oxidation migrate towards the cathode, through
45 an external circuit, where they combine with oxygen and protons to form water. sMFC that employ
46 paddy soil has gained considerable attention recently because of the unique biological and
47 chemical characteristics of paddy soil make them ideal for power production [5]. In addition to
48 power generation, sMFC have also found use in stimulating soil bioremediation. For instance, the
49 anode of the sMFC can serve as an electron sink for anode respiring bacterial (ARB) and accelerate
50 the bioremediation of both polycyclic aromatic hydrocarbons and redox active heavy metals [6,7].

51 However, sMFC deployment in paddy fields has been shown to alter soil bacterial
52 community structure and abiotic components [8,9]. When an anode of sMFC is embedded into
53 anaerobic soils, it functions as a continuous sink for electrons and this alters soil chemistry [10,11].
54 This in turn increases soil *Eh*, decreases soil pH and changes the bioavailability of soil nutrients
55 such as phosphate and nitrogen [1,12]. Therefore these changes in soil chemistry may influence
56 the soil bacterial community composition, since soil *Eh*, pH and nutrient bioavailability are the
57 major drivers of soil bacterial community structure [13-15]. Furthermore, the sMFC have also been
58 used to prevent the deterioration of overlying water quality and for the removal or stabilization of
59 toxic heavy metals [7,16,17]. Previous studies have shown that sMFC can be used as a mitigation
60 technology in soils contaminated with chromium, uranium, cadmium, lead or copper [7,17,18].

61 Anode bacterial community determines the capability of the sMFC to function effectively

62 as a remediation technology. For example, when non-anode respiring bacteria are abundant in the
63 anode chamber, these microbes may compete with ARB for resources, thereby limiting the
64 performance of the sMFC. However, regulating the anode potential has been shown to effectively
65 tailor the desired ARB consortium and suppress the growth of undesirable microbes, such as
66 methanogens [9,19]. This occurs because the anode potentials determine the accessibility of
67 electron ARB received for growth and development [20]. Thus at certain anode potential, ARB
68 are able to gain higher energy for growth from respiring the anode and out compete methanogens
69 for OM [19].

70 Moreover, adjusting applied external resistance (ER) in sMFC has also been shown to
71 affect the metabolic rate of ARB on the anode [21]. Previous studies have demonstrated that
72 decreasing ER increases the oxidative degradation of OM and the current output from the sMFC
73 [3]. Furthermore, the current produced by the sMFC can also stimulate microbiological oxidation
74 of soil OM by fermentative bacteria [6,22]. Even though, several studies have examined the
75 influence of the anode potentials on the biofilm community composition in double chamber MFC,
76 to date there is no universal consensus on the effect of the anode potential on the anode community
77 structure. Although the application of sMFC is increasing, studies examining the effect of anode
78 potential on sMFC community have received limited to no attention. Torres, *et al.* [20], observed
79 selective enhancement of *Geobacter sulfurreducens* at lower anode potentials (-0.15V , -0.09V ,
80 and 0.02V vs SHE) and an increase in bacterial diversity at higher anode potential (0.37V). On the
81 contrary, Zhu, *et al.* [23] argues that anode community is unaffected by anode potential and that
82 the electrogenic communities acclimatize to different anode potentials. Nonetheless, to date, few
83 studies have been done to examine the influence of the anode at different ER on soil biotic and
84 abiotic constituents collectively.

85 Thus, the objectives of this study are, therefore, to examine the effects of different ER on
86 soil and anode bacterial community structure, OM removal efficiency and selective soil metal
87 behavior at various resistances away from the anode. The results from this study suggest that lower
88 ER can be used to selectively enhance ARB abundance and increase OM removal.

89 **2. Materials and Methods**

90 **2.1. Paddy soils sample**

91 The paddy soil (0–15 cm below the soil–water interface) samples were collected from a
92 rice paddy in Qiyang, Hunan (GPS N26.760 E111.86) and transported directly to the laboratory.
93 These samples were then air-dried and sieved to 2 mm to remove all coarse debris. The soil
94 properties, including texture, pH, OM content, arsenic (As) and Iron (Fe) were measured to be clay,
95 6, 23.2g/kg, 73.7mg/kg and 53.69 g/kg, respectively.

96 **2.2. Soil Microbial Fuel Cell assembly**

97 Eighteen sMFC were constructed from the paddy soil and operated at different ER 2000 Ω ,
98 1000 Ω , 200 Ω , 80 Ω and 50 Ω in triplicates for 90 days. Of the eighteen sMFC three were controls,
99 the anodes and cathodes were not connected (open circuit). All sMFC were constructed according
100 to a previously reported method by Wang, *et al.* [24] with slight modifications. Briefly, a columnar
101 polyethylene terephthalate container (10 cm diameter \times 15 cm depth) with two valve ports (~2 cm
102 above the anode and adjacent to the anode) was used to construct each sMFC. Circular carbon felts
103 with geometric surface area of 50.2 cm² were used as anodes and cathodes. A data logger (USB-
104 7660B, ZTIC, China) was used to record the voltage between the anode and cathode.

105 Using 700 g (dry weight) of soil sample, ~1 cm depth of soil was placed at the bottom of
106 the sMFC container. Then, the anode was placed on the surface of the soil layer and then buried
107 with additional soil to simulate anaerobic conditions. The cathode was placed above the soil in

108 aerobic conditions (half submerged in water and the other half in the open air). Deionized water
109 (1L) was added to flood the paddy soil.

110 **2.3. Chemical Analysis**

111 Each constructed sMFC was equipped with a self-made soil pore water sampler. The
112 sampler was made from a 0.45 μm hollow fiber membrane, which was inserted into the soil
113 through the valve port adjacent to the anode and 2 cm above the anode. The soil porewater was
114 sampled and analyzed for As and Fe by inductively coupled plasma emission spectrometry
115 (ICPMS) (NexlonTM 350x, Pekin Elmer, USA) and atomic absorption spectrometry (AAS)
116 (PinAAcleTM 900, PerkinElmer, USA), respectively. Dissolved organic carbon (DOC)
117 concentration was determined with a TOC analyzer (Shimadzu TOC-VCPH, Japan). The loss on
118 ignition (LOI) carbon content was determined gravimetrically. LOI was calculated according to
119 the following equation 1:

$$120 \text{ LOI (\%)} = ((D105 - D550)/D105) * 100 \quad (1)$$

121 where D105 is the dry mass of the sample heated 105 °C for 12 hours and D550 is the dry mass of
122 the sample after 4 hours of incubation at 550 °C. Samples were allowed to cool to room temperature
123 in a desiccator before determining D550.

124 **2.4. Bacterial Community Analysis**

125 Total Genomic DNA was extracted from the anode vicinity and bulk soil using the
126 PowerSoil DNA isolation kit (Mo Bio Laboratories, Inc., Carlsbad, CA) from all of the treatments
127 including the controls according to the manufacturer's protocol. The quantity of DNA in the
128 extracts was measured at 260 nm using a Qubit 2.0 Fluorometer (Invitrogen, Carlsbad, CA). The
129 DNA quality was verified by agarose gel electrophoresis. The DNA samples were stored at -80 °C
130 until sequencing.

131 The V3-V5 hypervariable regions of the 16S ribosomal RNA (rRNA) gene in bacteria were
132 amplified using primer pair 515f/907R [25,26]. The library preparations and Illumina MiSeq
133 sequencing of the 16S rRNA gene amplicon were outsourced to GENEWIZ, Inc. (Suzhou, China).
134 FLASH was used to merge paired-end reads and QIIME (Quantitative Insights Into Microbial
135 Ecology) (V1.7.0) was employed to optimize the data by removing low-quality sequence and for
136 all taxonomy analysis [27]. The low-quality reads were discarded. Subsequently, the sequences
137 were compared with the reference database (RDP Gold database) using UCHIME algorithm to
138 detect chimeric sequence, and then the chimeric sequences were removed [28,29]. The clean
139 sequences were clustered into operational taxonomic units (OTUs) (97% similarity) by UPARSE.
140 The phylogenetic taxonomy were assigned according to the Ribosomal Database Program (RDP)
141 classifier (Version 2.2) and the Green Genes Database at confidence threshold of 80% [28,30].

142 **2.5. Statistical Analysis**

143 One-way analysis of variance (ANOVA) was performed to test significant differences
144 between treatments using SPSS software (IBM SPSS Statistics 23.0) and OriginPro (Inc.,
145 OringinLab, USA). Tukey's honest significant difference (HSD) studentized range tests were
146 applied to differentiate between various treatments and a $p < 0.05$ was considered significant.
147 Alpha diversity indexes were calculated using Faith's phylogenetic diversity, Shannon diversity
148 index and the Chao1 richness estimator using QIIME. Beta diversity was assessed using principal
149 coordinate analysis (PCoA) and non-metric multidimensional scaling (NMDS) analysis.

150 **2.6 Nucleotide sequence accession number**

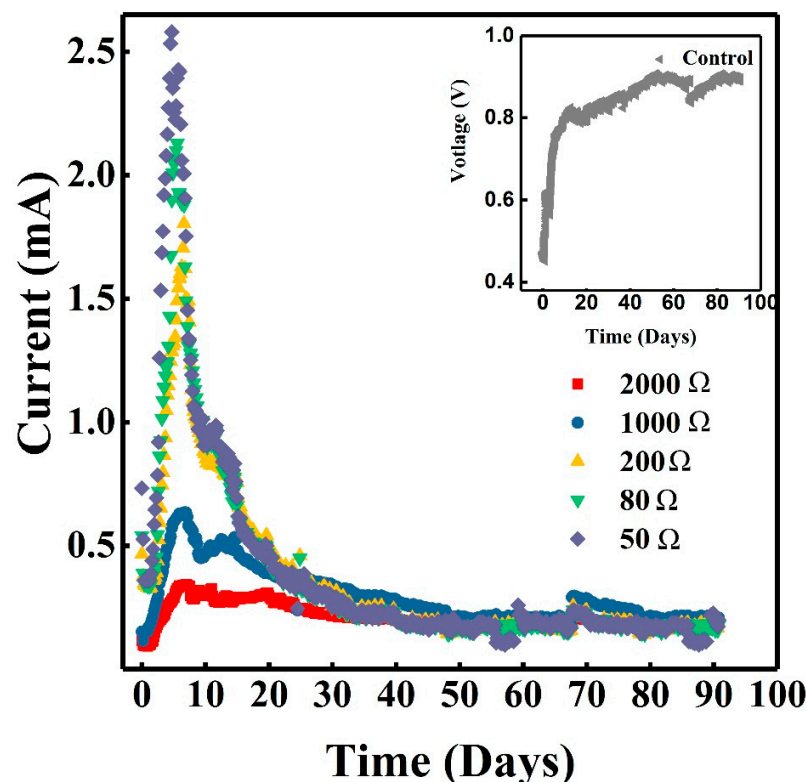
151 Nucleotide sequences were all deposited in the GeneBank database with accession numbers
152 MG814044 - MG815131.

153

154 3. Results

155 3.1. Electricity generation from soil MFCs with different external resistors

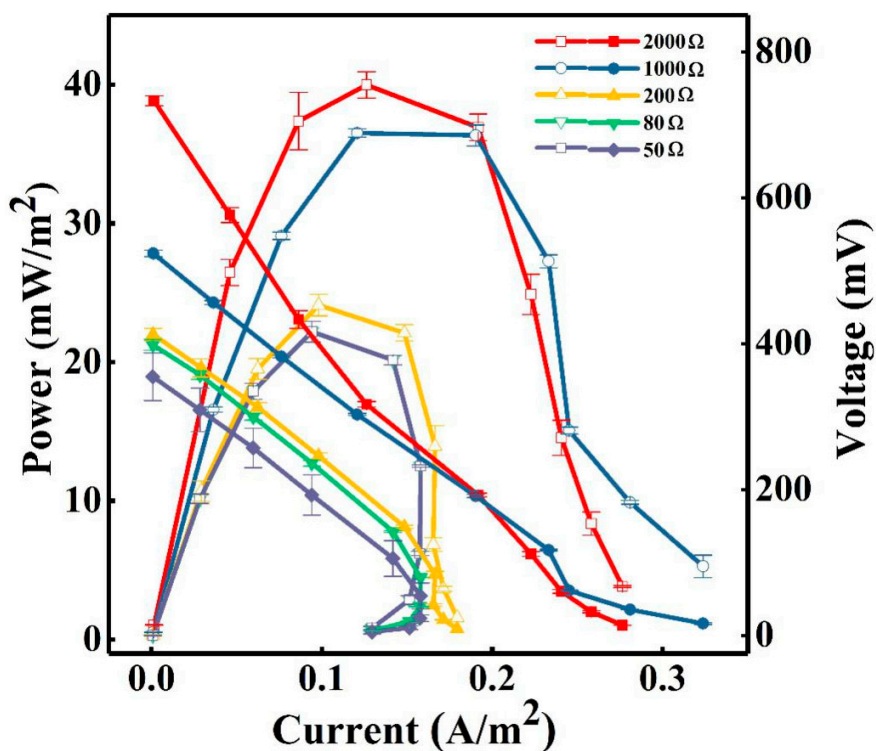
156 In this study each sMFC was loaded with a fixed resistor for the duration of the experiment.
157 Five different ER were tested 50 Ω , 80 Ω , 200 Ω , 1000 Ω and 2000 Ω and the current production
158 from the sMFC for 90 days of operation are illustrated in Figure 1. The current of the all sMFC
159 sharply increased during the initial stage regardless of ER and reached a maximum current at
160 around 10 days. The highest current produced was observed at an ER of 50 Ω (2.4mA), followed
161 by those of 80 Ω (2.1 mA), 200 Ω (1.6 mA) and 1000 Ω (0.8 mA). An ER of 2000 Ω produced the
162 lowest current (0.3mA). However after ca. 30 days all the current outputs irrespective of ER were
163 approximately the same (0.15-0.2 mA). The insert in Figure 1 shows change in the controls voltage
164 with time.



166 **Figure 1.** Current production from sMFC fixed with different external resistances during a 90-
167 day operation. The insert represent the change in the control's voltage with time.

168 **3.2. Polarization properties of the sMFC**

169 The power current curve is an important attribute used to determine the performance of
170 MFC. The power current curves in this study were obtained by varying ER from 10K Ω to 10 Ω
171 and are compared in Figure 2. The power densities of the sMFC set at 1000 Ω and 2000 Ω ER
172 were similar and those set at lower ER (50 Ω , 80 Ω and 200 Ω) mirrored each other. As shown in
173 Figure 2, the maximum power density observed in the sMFC at different resistance were 22.2,
174 22.2, 24.1, 36.5 and 40.0 mW/m² for 50 Ω , 80 Ω , 200 Ω , 1000 Ω and 2000 Ω respectively. Similarly,
175 the polarization slope method was used to determine the ohmic resistance for each sMFC. The
176 results followed a similar trend to maximum power except for the case of 200 Ω . The 50 Ω ER
177 had the lowest ohmic resistance and 2000 Ω had the highest ohmic resistance. The ohmic resistance
178 increased in the following order 50 (389 Ω) < 80 (390 Ω) < 1000 (476 Ω) < 200 (556 Ω) < 2000
179 (572 Ω).



180

181 **Figure 2.** Power density (filled symbols) and polarization curves (open symbols) of sMFCs. The
 182 error bars represent standard error of measured concentrations of triplicate samples.

183 The anode and cathode potentials (versus Ag/AgCl reference electrode) for each sMFC at
 184 different ER are shown in Figure S1. In general, the anode potential became more positive with
 185 decreasing ER, however there was negligible difference between the potential of the anode at 50
 186 Ω, 80 Ω and 200 Ω. The working potential of the anode for the sMFC with an ER of 2000 Ω was
 187 much lower than those with other ER, approximately 345 mv lower than those with ER of 50 Ω,
 188 80 Ω and 200 Ω. Moreover, the highest cathodic potential was observed in the sMFC with 200 Ω
 189 ER followed by that of 80 Ω and 1000 Ω. The cathodic potential of sMFC with ER of 50 Ω and
 190 2000 Ω were approximately the same. These findings indicate that the cathode was responsible for
 191 the difference in sMFC performance with different ER, especially at ER of 200 Ω, 80 Ω and 50 Ω

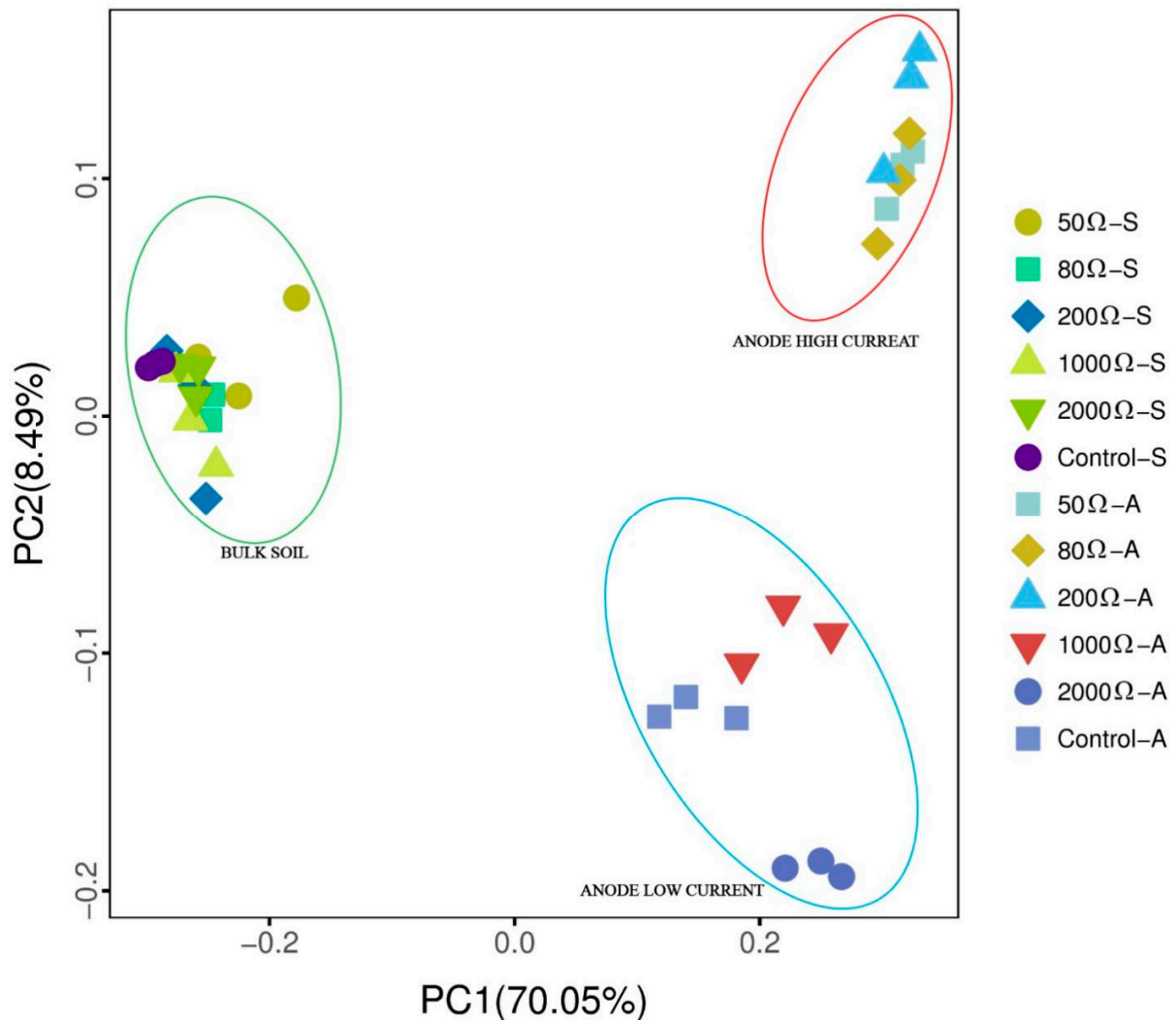
192 [3]. This is due to the sharp decrease in cathode potential with decreasing resistance compared to
193 that of the anode.

194 **3.3. Bacterial community structure**

195 The Illumina MiSeq sequencing of the 16S rRNA gene yielded a total of 2164539 bacterial
196 sequences (average read length 450 bp). The valid reads clustered into 1162 OTUs at a 3% distance.
197 The rarefaction analysis showed a clear saturation trend indicating that the sequencing depth of
198 30,000 was sufficient (Figure S2). The notion of sufficient depth being met was also supported by
199 the high Good's Coverages (>0.99) (Table S1). The observed alpha diversity indices showed that
200 the bacterial communities in the vicinity of the anode were less diverse than that of the bulk soil
201 and that applying different ER had a negligible influence on bacterial diversity (Table S1).

202 Beta diversity indices PCoA (Figure 3) and NMDS (Figure S3) analysis of the bacterial
203 community composition, reveal three distinctive clusters. Where the bulk soils bacterial
204 community clustered together regardless of applied ER, while the samples from anode vicinity
205 posed at high ER (1000 Ω and 2000 Ω) clustered with the control and that of the lower resistances
206 (50 Ω , 80 Ω and 200 Ω) formed another cluster. These findings demonstrate that the ER may shape
207 the bacterial communities that develop in the anode vicinity but have minimal effect on that of the
208 bulk soil.

209

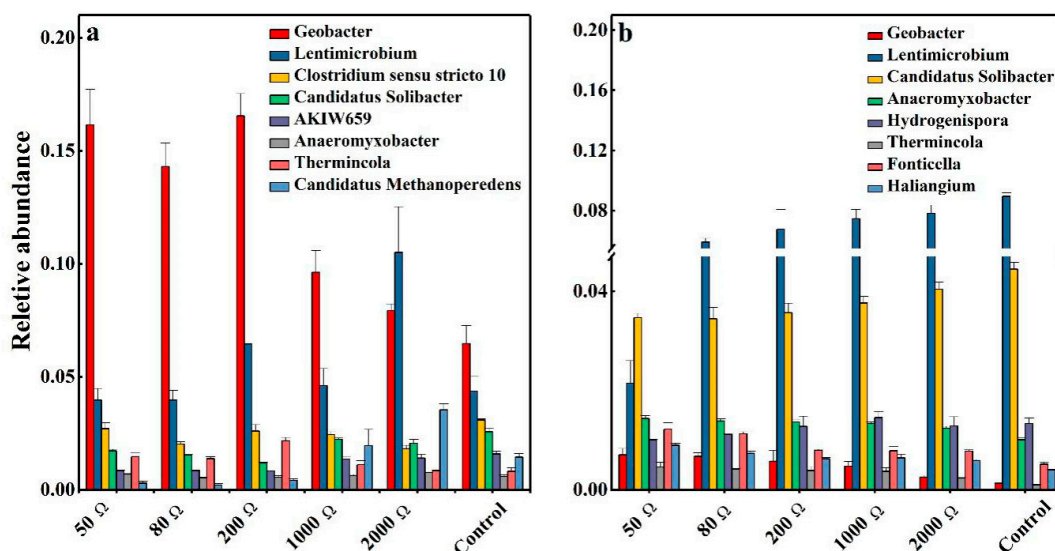


210

211 **Figure 3.** Principal Coordinates Analysis (PCoA) of the sMFC and controls bacterial community
 212 composition based on the unweighted UniFrac distance matrix. The x- and y-axes are indicated
 213 by the first and second coordinates, respectively, and the values in parentheses show the
 214 percentages of the community variation explained.

215 Phylum and class level analysis reveal that fourteen bacterial phyla and fourteen bacterial
 216 classes made up the vast majority of total 16S rRNA gene sequences, accounting for 92% and 78%
 217 of total reads, respectively. Taxonomic classification at the phylum showed that the phyla

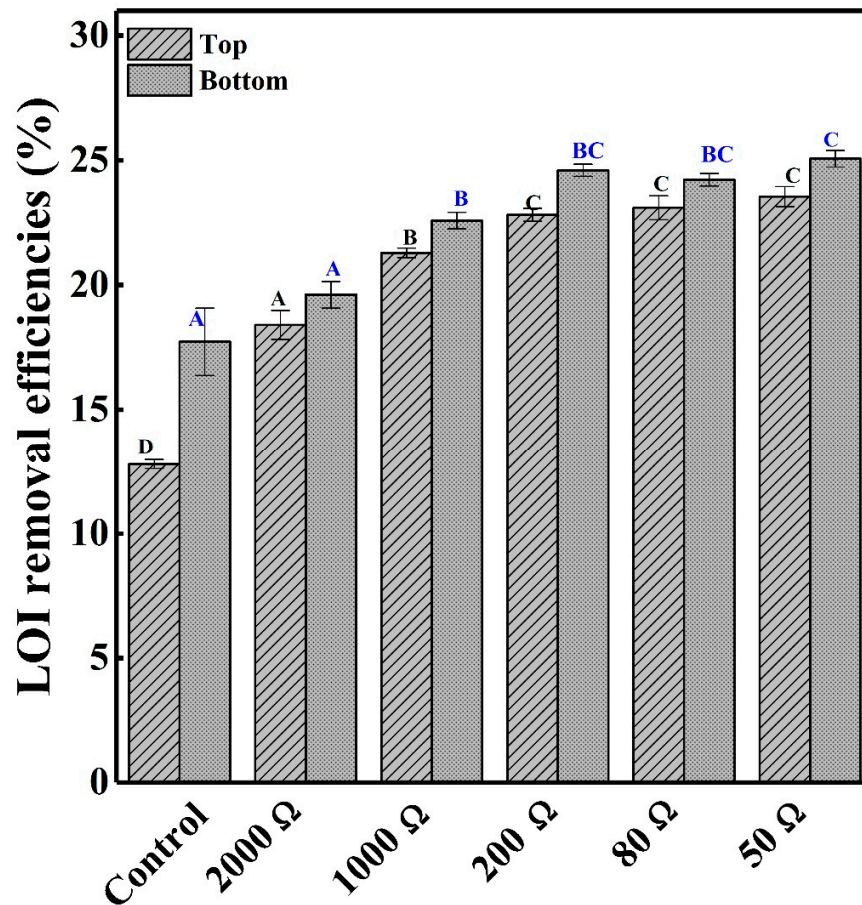
218 *Proteobacteria*, *Chloroflexi*, *Nitrospirae* and *Chlorobi* were enhanced with decreasing ER and
 219 *Bacteroidetes*, *Acidobacteria* and *Euryarchaeota* were suppressed (Figure S4). The relative
 220 abundance of *Proteobacteria* in the anode biofilms were 29.7% (50 Ω), 26.5% (80 Ω), 27.2% (200
 221 Ω), 23.2% (1000 Ω), 22.6% (2000 Ω) and 21.3% (control) respectively, when *Chloroflexi*
 222 accounted for 10.8% (50 Ω), 11.7% (80 Ω), 11.5% (200 Ω), 10.3% (1000 Ω), 8.04% (2000 Ω) and
 223 9.86% (control). The relative abundance of *Nitrospirae* and *Chlorobi* followed a similar trend 11.5
 224 and 2.56 % (50 Ω), 14.1 and 2.36% (80 Ω), 13.9 and 1.64% (200 Ω), 8.01 and 1.06% (1000 Ω),
 225 7.00 and 1.34% (2000 Ω) and 5.2 and 0.86% (control) respectively. Analysis on the class level
 226 showed that *Deltaproteobacteria*, *Bacteroidetes vadinHA17*, *Nitrospira* and *Subgroup18* were
 227 strongly influenced by ER. Further analysis at the genus level showed that the *Geobacter* and
 228 *Lentimicrobium* were most influence genus. *Geobacter* was enhanced with decreasing ER in both
 229 the bulk soil and the anode vicinity, while in the bulk soil *Lentimicrobium* was suppressed (Figure
 230 4).



231
 232 **Figure 4.** Relative abundance of bacterial community composition at genus level (a) anode
 233 vicinity and (b) bulk soil.

234 **3.4. Organic matter removal**

235 The loss on ignition (LOI) value was used as a proxy to estimate the OM content in the soil
236 and its removal efficiency was used to analyze the effect of ER on degradation of organic carbon
237 by the sMFC. Figure 5 illustrates the removal efficiency of LOI from the soil samples at two
238 distances (~1cm and 2cm) away from the anode at different ER. The removal efficiency of LOI
239 increased with decreasing ER and distance away from the anode. The removal efficiency of LOI
240 in the vicinity of the anode were 2.0%, 4.9%, 6.9% and 7.4% higher than the control, for sMFC
241 loaded with 2000 Ω , 1000 Ω , 200 Ω , 80 Ω and 50 Ω ER, respectively. A similar trend was observed
242 in the removal efficiency of OM in the bulk soil. A significantly ($p < 0.05$) higher removal
243 efficiency of LOI irrespective of location was observed between the control and all the treatments
244 except for 2000 Ω (anode vicinity). The results obtained here demonstrate that the anode could
245 enhance bacterial oxidation of organics and decreasing ER can further promote this process.



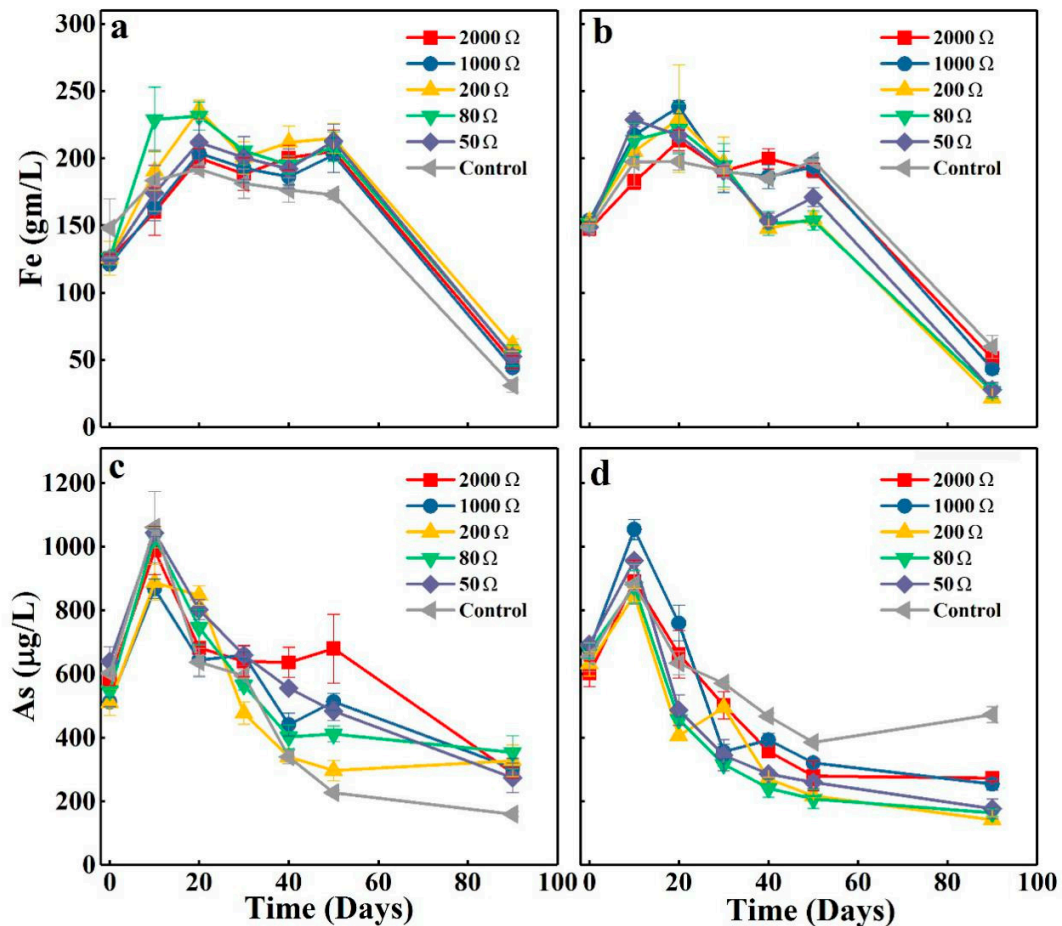
246

247 **Figure 5.** Removal efficiencies of lost on ignition carbon. The error bars represent standard error
 248 of measured concentrations of triplicate samples. Different letters represent statistical
 249 significance.

250 3.5. Changes of porewater As, Fe and Ni

251 The concentrations of As, Fe and Ni in the bulk soil porewater and in the anode vicinity
 252 were tested at intervals of 10 days from day 0-60 and then tested at the end of 90 days (Figure 6a-
 253 d and Figure S5a-b). As seen in Figure 6a-b and Figure S5a-b no significant ($p > 0.05$) differences
 254 was observed in bulk soil porewater for As, Fe and Ni with time irrespective of ER, however the
 255 concentration of both Fe and As was slightly elevated in the treatments compared to the controls
 256 at the end of 90 days. In the vicinity of the anode the concentration of As, Fe and Ni were lower

257 in the treatments compared to the control. In general the concentration of these metals decrease
 258 with decreasing ER in the anode vicinity.



259
 260 **Figure 6.** Fe and As variation in soil porewater along with incubation time. Panels a and b
 261 represent Fe concentration in the bulk soil and anode vicinity respectively. Panels c and d
 262 represent As concentration in the bulk soil and anode vicinity respectively. The error bars
 263 represent standard error of measured concentrations of triplicates samples.

264 4. Discussion

265 Various studies have shown that the applied ER can greatly affect the current production,
 266 because ER plays an important role in the enrichment process of ARB on the anode [21,31]. These

267 studies revealed that low resistance stimulate ARB growth on the anode and thereby improved
268 current production. As illustrated in Figure 1, the rapid initial increase in current occurred as a
269 result of the high readily oxidized organic content of the soil and the accumulation of the
270 electrochemically active biofilm on the anode (i.e. *Geobacter*). The steady decrease in voltage
271 observed after day 10 can be attributed to reduction in the physiological activity of the ARB on
272 the anode and cathode limitations. The different intensity observed in current peak, occurring at
273 different ER, was probably due to the increase in internal resistance with increasing ER (Figure 2).
274 The results obtained here are in accordance with that of Hong, *et al.* [32] and Holmes, *et al.* [33].
275 In both studies a maximum current was achieved within 10-20 days which was followed by a
276 gradual decrease in current production with time.

277 The increase in current with lower ER led to the higher removal efficiency of LOI in
278 treatments fixed at low ER due to stimulated increase of anaerobe metabolic activities (Figure 5).
279 Previous studies have shown that current can accelerate the metabolic reaction rate in anaerobic
280 bacteria by enhancing the release of enzymes and altering the permeability of anaerobes cell
281 membrane [6,22]. Thus, increase in electron transfer rate from anode to cathode due to lower ohmic
282 resistance improved bacterial metabolism of both the anaerobic bacteria in the anode vicinity and
283 the bulk soil. This consequently led to the higher removal of OM by the sMFC with the 50 Ω , 80
284 Ω , and 200 Ω and 1000 Ω circuit load. The relatively lower current at 2000 Ω circuit load results
285 in minimal OM removal compared to the control. The increase in current and decrease in OM
286 content in the treatment are probably responsible for the slightly lower concentration of As, Fe and
287 Ni in the anode vicinity. Studies have shown that organic carbon is the main electron donor for
288 anaerobic reduction of Fe oxide minerals bearing metals and metalloids. A positive correlation has
289 also been observed between Fe and As mobilization and DOC bioavailability [34]. Moreover, the

290 reduction of Ni in the anode vicinity of the treatment was probably due to electromigration and
291 immobilization of Ni on the anode [35].

292 The effect of different ER on bacterial community structure enriched in the bulk soil and
293 the anode vicinity of the sMFC after 90 days of operation revealed that differences in community
294 profiles in the vicinity of the anode and minor changes in that of the bulk soils. As shown in the
295 PCoA analysis (Figure 3) and NMDS (Figure S3) the anode community can be divided into two
296 groups. Samples taken from the anode vicinity with lower circuit loads (50 Ω , 80 Ω and 200 Ω i.e.
297 high current) were similar and those from higher ER (1000 and 2000 Ω i.e. low current) were more
298 comparable to the control. The results observed here suggested that distinct bacterial communities
299 developed at different current densities.

300 The similarity in anode potential in groups with lower or higher ER could be reason for the
301 observed pattern. Numerous studies have shown that bacterial community varied depending on the
302 anode potentials [21,36]. In addition the anode has been shown to accelerate the metabolic rate
303 and development of electroactive bacterial community in its vicinity [21,36]. In a study on the
304 effects of ER on the anode [21], observed higher anode potential and columbic efficiency with
305 lower ER. The authors concluded that lower ER produce higher current and that ER can be used
306 to control anode potential and for the selection of ARB. Thus, it could be assumed that higher ER
307 possibly limited ARB colonization and metabolic activities on the anode and vice versa when ER
308 were reduced.

309 Moreover taxonomical analysis of the anode community indicated that reducing ER
310 enhances ARB such as *Deltaproteobacteria* and *Nitrospira* (Figure S4). This occurred because
311 when ARB uses anode at higher electrochemical potentials these ARB obtain more energy [36,37].
312 Thus, at lower ER higher current generation and relative abundance of ARB was observed.

313 Previous studies have demonstrated that the *Geobacter* sp. current generation properties and
314 growth are strongly affected by the anode potentials [38,39]. Torres, *et al.* [20] investigated the
315 bacterial community at different anode potential and found that lower anode potential had a high
316 selection of the *Geobacter* sp., since they are able to transfer electrons to the anode efficiently with
317 minimal energy loss. These results are in line with our findings where *Geobacter* relative
318 abundance increased with decreasing ER (Figure 4). The results obtained here demonstrates that
319 ER can significantly influence the composition of anode bacterial communities by selectively
320 enhancing electrogenic bacteria.

321 5. Conclusion

322 In this study the effect of different ER on the sMFC performance, OM removal and
323 bacterial community composition was investigated. The results indicated significant influences of
324 ER on current production, OM removal efficiency and bacterial diversity. In particular, greater
325 current densities, OM removal efficiencies and enhancement of *Geobacter* were observed at lower
326 ER (50 Ω , 80 Ω and 200 Ω). The current study illustrates that lower ER can be used to selectively
327 enhance ARB relative abundance and increase OM removal efficiencies while decreasing metal
328 concentration in soil porewater.

329 **Supplementary Materials:** The following are available online at www.mdpi.com. Table S1.
330 Similarity-based OTUs and species richness and diversity estimates, Figure S1. Anode and cathode
331 polarization curves. The error bars represent standard error of measured concentrations of triplicate
332 samples, Figure S2. Rarefaction curves based on MiSeq sequencing of bacterial communities
333 showing the diversity of OTUs (similarity cut off of 97%). OTUs, Operational Taxonomic Units,
334 Figure S3. Non-metric multidimensional scaling (NMDS) analysis of the sMFC and controls
335 bacterial community composition based on Bray–Curtis dissimilarity matrix for bacterial

336 communities that consisted of OTUs (97% similarity level), Figure S4. Relative abundance of
337 microbial community composition at phylum ((a) anode vicinity and (b) bulk soil) and class level
338 ((a) anode vicinity and (b) bulk soil), Figure S5. Nickel variation in soil porewater along with
339 incubation time. a and b represent nickel concentration in the bulk soil and anode vicinity
340 respectively. The error bars represent standard error of measured concentrations of triplicates
341 samples.

342 **Author Contributions:** Williamson Gustave, Zhao-Feng Yuan and Zheng Chen conceived,
343 designed, and performed the experiments with support from Yu-Xiang Ren and Hu-Cheng Chang.
344 Williamson Gustave and Zhao-Feng Yuan and Zheng Chen worked together to analyze the data.
345 Williamson Gustave, Zhao-Feng Yuan and Zheng Chen wrote the paper with edits from Raju Sekar.
346 All authors read and approved the content.

347 **Acknowledgement:** This work was supported by the National Science Foundation of China
348 (41571305) and Jiangsu Science and Technology Program (BK20161251). The authors
349 acknowledge the kind help of Zhou Xiao and Yi-Li Cheng for their technical support in the sample
350 analysis. The authors are grateful to Markus Klingelfuss and Jacquelin St. Jean for proof reading
351 the manuscript. The authors are also grateful to Elmer Villanueva for his help in the statistical
352 analysis.

353 **Conflicts of Interest:** The authors declare no conflict of interest.

354

355 **References**

- 356 1. Hong, S.W.; Chang, I.S.; Choi, Y.S.; Kim, B.H.; Chung, T.H. Responses from freshwater
357 sediment during electricity generation using microbial fuel cells. *Bioprocess. Biosyst. Eng.*
358 **2009**, *32*, 389-395. DOI: 10.1007/s00449-008-0258-9
- 359 2. De Schampelaire, L.; Rabaey, K.; Boeckx, P.; Boon, N.; Verstraete, W. Outlook for
360 benefits of sediment microbial fuel cells with two bio-electrodes. *Microb. Biotechnol.* **2008**,
361 *1*, 446-462. DOI: 10.1111/j.1751-7915.2008.00042.x
- 362 3. Song, T.S.; Yan, Z.S.; Zhao, Z.W.; Jiang, H.L. Removal of organic matter in freshwater
363 sediment by microbial fuel cells at various external resistances. *J. Chem. Technol.*
364 *Biotechnol.* **2010**. DOI: 10.1002/jctb.2454
- 365 4. Chen, Z.; Huang, Y.C.; Liang, J.H.; Zhao, F.; Zhu, Y.G. A novel sediment microbial fuel
366 cell with a biocathode in the rice rhizosphere. *Bioresour. Technol.* **2012**, *108*, 55-59. DOI:
367 10.1016/j.biortech.2011.10.040
- 368 5. Kaku, N.; Yonezawa, N.; Kodama, Y.; Watanabe, K. Plant/microbe cooperation for
369 electricity generation in a rice paddy field. *Appl Microbiol. Biotechnol.* **2008**, *79*, 43-49.
370 DOI: 10.1007/s00253-008-1410-9
- 371 6. Yu, B.; Tian, J.; Feng, L. Remediation of pah polluted soils using a soil microbial fuel cell:
372 Influence of electrode interval and role of microbial community. *J. Hazard. Mater.* **2017**,
373 *336*, 110. DOI: 10.1016/j.jhazmat.2017.04.066
- 374 7. Wang, C.; Deng, H.; Zhao, F. The remediation of chromium (vi)-contaminated soils using
375 microbial fuel cells. *Soil Sediment Contam.* **2015**, *25*, 1-12. DOI:
376 10.1080/15320383.2016.1085833

- 377 8. Lu, L.; Huggins, T.; Jin, S.; Zuo, Y.; Ren, Z.J. Microbial metabolism and community
378 structure in response to bioelectrochemically enhanced remediation of petroleum
379 hydrocarbon-contaminated soil. *Environ. Sci. Technol.* **2014**, *48*, 4021. DOI:
380 10.1021/es4057906
- 381 9. Kouzuma, A.; Kaku, N.; Watanabe, K. Microbial electricity generation in rice paddy fields:
382 Recent advances and perspectives in rhizosphere microbial fuel cells. *Appl. Microbiol.*
383 *Biotechnol.* **2014**, *98*, 9521-9526. DOI: 10.1007/s00253-014-6138-0
- 384 10. Logan, B.E. *Microbial fuel cells*. A John Wiley & Sons, Inc.: 2008.
- 385 11. Huang, D.Y.; Zhou, S.G.; Chen, Q.; Zhao, B.; Yuan, Y.; Zhuang, L. Enhanced anaerobic
386 degradation of organic pollutants in a soil microbial fuel cell. *Chem. Eng. J.* **2011**, *172*,
387 647-653. DOI: 10.1016/j.cej.2011.06.024
- 388 12. Touch, N.; Hibino, T.; Morimoto, Y.; Kinjo, N. Relaxing the formation of hypoxic bottom
389 water with sediment microbial fuel cells. *Environ. Technol.* **2017**, 1-25. DOI:
390 10.1080/09593330.2017.1285965
- 391 13. Nicol, G.W.; Leininger, S.; Schleper, C.; Prosser, J.I. The influence of soil pH on the
392 diversity, abundance and transcriptional activity of ammonia oxidizing archaea and
393 bacteria. *Environ. Microbiol.* **2008**, *10*, 2966-2978. DOI: 10.1111/j.1462-
394 2920.2008.01701.x
- 395 14. Wu, Y.; Zeng, J.; Zhu, Q.; Zhang, Z.; Lin, X. Ph is the primary determinant of the bacterial
396 community structure in agricultural soils impacted by polycyclic aromatic hydrocarbon
397 pollution. *Sci. Rep.* **2017**, *7*, 40093. DOI: 10.1038/srep40031

- 398 15. Pettridge, J.; Firestone, M.K. Redox fluctuation structures microbial communities in a wet
399 tropical soil. *Appl. Environ. Microbiol.* **2005**, *71*, 6998-7007. DOI:
400 10.1128/aem.71.11.6998-7007.2005
- 401 16. Zhou, Y.; Jiang, H.; Cai, H. To prevent the occurrence of black water agglomerate through
402 delaying decomposition of cyanobacterial bloom biomass by sediment microbial fuel cell.
403 *J. Hazard. Mater.* **2015**, *287*, 7-15. DOI: 10.1016/j.jhazmat.2015.01.036
- 404 17. Chen, Z.; Zhu, B.-K.; Jia, W.-F.; Liang, J.-H.; Sun, G.-X. Can electrokinetic removal of
405 metals from contaminated paddy soils be powered by microbial fuel cells? *Environ.*
406 *Technol. Innov.* **2015**, *3*, 63-67. DOI: 10.1016/j.eti.2015.02.003
- 407 18. Abbas, S.Z.; Rafatullah, M.; Ismail, N.; Syakir, M.I. A review on sediment microbial fuel
408 cells as a new source of sustainable energy and heavy metal remediation: Mechanisms and
409 future prospective. *Int. J. Energ. Res.* **2017**, *41*, 1242-1264. DOI: 10.1002/er.3706
- 410 19. Jung, S.; Regan, J.M. Influence of external resistance on electrogenesis, methanogenesis,
411 and anode prokaryotic communities in microbial fuel cells. *Appl. Environ. Microbiol.* **2011**,
412 *77*, 564-571. DOI:10.1128/aem.01392-10
- 413 20. Torres, C.I.; Krajmalnikbrown, R.; Parameswaran, P.; Marcus, A.K.; Wanger, G.; Gorby,
414 Y.A.; Rittmann, B.E. Selecting anode-respiring bacteria based on anode potential:
415 Phylogenetic, electrochemical, and microscopic characterization. *Environ. Sci. Technol.*
416 **2009**, *43*, 9519-9524. DOI: 10.1021/es902165y
- 417 21. Rismani-Yazdi, H.; Christy, A.D.; Carver, S.M.; Yu, Z.; Dehority, B.A.; Tuovinen, O.H.
418 Effect of external resistance on bacterial diversity and metabolism in cellulose-fed
419 microbial fuel cells. *Bioresour. Technol.* **2011**, *102*, 278-283. DOI:
420 10.1016/j.biortech.2010.05.012

- 421 22. Pitts, K.; Dobbin, P.S.; Reyesramirez, F.; Thomson, A.J.; Richardson, D.J.; Seward, H.E.
422 Characterization of the *Shewanella oneidensis* mr-1 decaheme cytochrome mtra expression
423 in *Escherichia coli* confers the ability to reduce soluble Fe(III) chelates. *J. Biol. Chem.*
424 **2003**, *278*, 27758-27765. DOI: 10.1074/jbc.M302582200
- 425 23. Zhu, X.; Yates, M.D.; Hatzell, M.C.; Rao, H.A.; Saikaly, P.E.; Logan, B.E. Microbial
426 community composition is unaffected by anode potential. *Environ. Sci. Technol.* **2014**, *48*,
427 1352-1358. DOI: 10.1021/es404690q
- 428 24. Wang, N.; Chen, Z.; Li, H.B.; Su, J.Q.; Zhao, F.; Zhu, Y.G. Bacterial community
429 composition at anodes of microbial fuel cells for paddy soils: The effects of soil properties.
430 *J. Soils Sediments* **2015**, *15*, 926-936. DOI: 10.1007/s11368-014-1056-4
- 431 25. Sun, W.; Xiao, E.; Dong, Y.; Tang, S.; Krumins, V.; Ning, Z.; Sun, M.; Zhao, Y.; Wu, S.;
432 Xiao, T. Profiling microbial community in a watershed heavily contaminated by an active
433 antimony (sb) mine in southwest china. *Sci. Total Environ.* **2016**, *550*, 297-308. DOI:
434 10.1016/j.scitotenv.2016.01.090
- 435 26. Xiao, E.; Krumins, V.; Xiao, T.; Dong, Y.; Song, T.; Ning, Z.; Huang, Z.; Sun, W. Depth-
436 resolved microbial community analyses in two contrasting soil cores contaminated by
437 antimony and arsenic. *Environ. Pollut.* **2016**, *221*, 244. DOI: 10.1016/j.envpol.2016.11.071
- 438 27. Caporaso, J.G.; Kuczynski, J.; Stombaugh, J.; Bittinger, K.; Bushman, F.D.; Costello, E.K.;
439 Fierer, N.; Pena, A.G.; Goodrich, J.K.; Gordon, J.I. Qiime allows analysis of high-
440 throughput community sequencing data. *Nat. Methods* **2010**, *7*, 335-336. DOI:
441 10.1038/nmeth.f.303

- 442 28. Wang, Q.; Garrity, G.M.; Tiedje, J.M.; Cole, J.R. Naïve bayesian classifier for rapid
443 assignment of rRNA sequences into the new bacterial taxonomy. *Appl. Environ. Microbiol.*
444 **2007**, *73*, 5261-5267. DOI: 10.1128/AEM.00062-07
- 445 29. Edgar, R.C.; Haas, B.J.; Clemente, J.C.; Quince, C.; Knight, R. Uchime improves
446 sensitivity and speed of chimera detection. *Bioinformatics* **2011**, *27*, 2194-2200. DOI:
447 10.1093/bioinformatics/btr381
- 448 30. Desantis, T.Z.; Hugenholtz, P.; Larsen, N.; Rojas, M.; Brodie, E.L.; Keller, K.; Huber, T.;
449 Dalevi, D.; Hu, P.; Andersen, G.L. Greengenes, a chimera-checked 16s rRNA gene database
450 and workbench compatible with arb. *Appl. Environ. Microbiol.* **2006**, *72*, 5069-5072. DOI:
451 10.1128/aem.03006-05
- 452 31. Mohan, S.V.; Mohanakrishna, G.; Reddy, B.P.; Saravanan, R.; Sarma, P. Bioelectricity
453 generation from chemical wastewater treatment in mediatorless (anode) microbial fuel cell
454 (MFC) using selectively enriched hydrogen producing mixed culture under acidophilic
455 microenvironment. *Biochem. Eng. J.* **2008**, *39*, 121-130. DOI:10.1016/j.bej.2007.08.023
- 456 32. Hong, S.W.; Chang, I.S.; Choi, Y.S.; Chung, T.H. Experimental evaluation of influential
457 factors for electricity harvesting from sediment using microbial fuel cell. *Bioresour.*
458 *Technol.* **2009**, *100*, 3029-3035. DOI: 10.1016/j.biortech.2009.01.030
- 459 33. Holmes, D.E.; Bond, D.R.; O'Neil, R.A.; Reimers, C.E.; Tender, L.R.; Lovley, D.R.
460 Microbial communities associated with electrodes harvesting electricity from a variety of
461 aquatic sediments. *Microb. Ecol.* **2004**, *48*, 178-190. DOI: 10.1007/s00248-003-0004-4
- 462 34. Wang, N.; Xue, X.; Juhasz, A.L.; Chang, Z.; Li, H. Biochar increases arsenic release from
463 an anaerobic paddy soil due to enhanced microbial reduction of iron and arsenic. *Environ.*
464 *Pollut.* **2017**, *220*, 514-522. DOI: 10.1016/j.envpol.2016.09.095

- 465 35. Giannis, A.; Pentari, D.; Wang, J.Y.; Gidakos, E. Application of sequential extraction
466 analysis to electrokinetic remediation of cadmium, nickel and zinc from contaminated soils.
467 *J. Hazard. Mater.* **2010**, *184*, 547-554. DOI: 10.1016/j.jhazmat.2010.08.070
- 468 36. Aelterman, P.; Freguia, S.; Keller, J.; Verstraete, W.; Rabaey, K. The anode potential
469 regulates bacterial activity in microbial fuel cells. *Appl. Microbiol. Biotechnol.* **2008**, *78*,
470 409-418. DOI: 10.1007/s00253-007-1327-8
- 471 37. Srikanth, S.; Mohan, S.V.; Sarma, P.N. Positive anodic poised potential regulates microbial
472 fuel cell performance with the function of open and closed circuitry. *Bioresour. Technol.*
473 **2010**, *101*, 5337-5344. DOI: 10.1016/j.biortech.2010.02.028
- 474 38. Srikanth, S.; Marsili, E.; Flickinger, M.C.; Bond, D.R. Electrochemical characterization of
475 *Geobacter sulfurreducens* cells immobilized on graphite paper electrodes. *Biotechnol.*
476 *Bioeng.* **2008**, *99*, 1065-1073. DOI: 10.1002/bit.21671
- 477 39. Wei, J.; Liang, P.; Cao, X.; Huang, X. A new insight into potential regulation on growth
478 and power generation of *Geobacter sulfurreducens* in microbial fuel cells based on energy
479 viewpoint. *Environ. Sci. Technol.* **2010**, *44*, 3187-3191. DOI: 10.1021/es903758m
- 480